CORA Cork Open Research Archive
Cartlann Taighde Oscailte Chorcaí

Title	Numerical simulation of the anodic formation of nanoporous InP
Authors	Lynch, Robert P.;O'Dwyer, Colm;Clancy, Ian;Corcoran, David;Buckley, D. Noel
Publication date	2004-01-01
Original Citation	Lynch, R., O'Dwyer, C., Clancy, I., Corcoran, D., Buckley, D. N. (2004) 'Numerical Simulation of the Anodic Formation of Nanoporous InP', 206th Meeting of the Electrochemical Society: State-of-the-Art Program on Compound Semiconductors XLI. Hilton Hawaiian Village, Honolulu, Hawaii, 3-8 October. Pennington, NJ: The Electrochemical Society, 6, pp. 85-95.
Type of publication	Conference item
Rights	© The Electrochemical Society, Inc. 2004. All rights reserved. Except as provided under U.S. copyright law, this work may not be reproduced, resold, distributed, or modified without the express permission of The Electrochemical Society (ECS). The archival version of this work was published in Lynch, R., O' Dwyer, C., Clancy, I., Corcoran, D., Buckley, D. N. (2004) 'Numerical Simulation of the Anodic Formation of Nanoporous InP', 206th Meeting of the Electrochemical Society: State -of-the-Art Program on Compound Semiconductors XLI. Hilton Hawaiian Village, Honolulu, Hawaii, 3-8 October. Pennington, NJ: The Electrochemical Society, 6, pp. 85-95.
Download date	2026-11-04 13:47:58
Item downloaded from	https://hdl.handle.net/10468/1008



UCC
University College Cork, Ireland
Coláiste na hOllscoile Corcaigh

NUMERICAL SIMULATION OF THE ANODIC FORMATION OF NANOPOROUS INDIUM PHOSPHIDE

R. Lynch, C. O'Dwyer, I. Clancy, D. Corcoran, and D. N. Buckley

Department of Physics, Materials & Surface Science Institute, University of Limerick, Ireland

ABSTRACT

Anodic etching of n-type InP in KOH electrolytes under suitable conditions leads to the formation of a nanoporous region beneath a ~40 nm dense near-surface layer [1]. The early stages of the process involve the formation of square-based pyramidal porous domains [2] and a mechanism is proposed based on directional selectivity of pore growth along the <100> directions. A numerical model of this mechanism is described in this paper. In the algorithm used the growth is limited to the <100> directions and the probability of growth at any pore tip is controlled by the potential and the concentration of electrolyte at the pore tip as well as the suitability of the pore tip to support further growth. The simulated porous structures and their corresponding current versus time curves are in good agreement with experimental data. The results of the simulation also suggest that, after an initial increase in current caused by the spreading out of the porous domains from their origins, growth is limited by the diffusion rate of electrolyte along the pores with the final fall-off in current being caused by irreversible processes such as the formation of a passivating film at the tips or some other modification of the state of the pore tip.

INTRODUCTION

Porosity in electrochemically etched semiconductors has been extensively investigated in the case of silicon and to a lesser degree in the case of III-V compounds such as GaAs [3,4] and InP [5-7]. It has been suggested that controlled modulation of the pore diameter and pore growth direction in semiconductors could allow for the fabrication of devices based on photonic crystal structures. In previous work by our group, the growth mechanism leading to sub-surface porosity in n-type InP, anodically etched in KOH [2], was experimentally investigated. It was observed that, in the early stages, pores originating from pits in the surface created porous domains with a square-based pyramidal structure beneath a thin (~40 nm) dense near-surface layer. The pore diameters, which can be controlled by varying the etching conditions, were also ~40 nm. These domains then merged into a continuous porous region beneath the dense near-surface layer, forming a relatively flat interface between the porous and bulk InP.

The mechanism proposed for the creation of these structures was based on pore growth selectively along the mutually orthogonal <100> directions at a growth rate which was homogeneous over each entire domain at any given time. This paper presents a numerical simulation of the proposed model using directional selectivity to restrict the growth of the structure with tip voltage and electrolyte concentration controlling the progression of growth at the pore tips. The system to be modeled consists of (100)-oriented S-doped n-type InP, with a carrier concentration of ~$4x10^{18}$ cm^{-3}, anodically etched under potentiostatic conditions in 5 mol dm^{-3} KOH electrolyte in darkness at room temperature. Experimentally measured potentials are referenced to a saturated calomel reference electrode (SCE).

NUMERICAL MODEL

The numerical model is based on a three dimensional cubic lattice with solid boundary conditions at the top surface layer, helical boundary conditions [8] for the vertical surface layers and a dynamic boundary at the bottom surface, which grows with the porous layer. The lattice lines (<100> directions) represent the paths along which pore growth can occur. Dimensionless parameters Ψ, r, τ and C are used to represent electrical potential, resistance, time and electrolyte concentration respectively. Pore growth originates through pits, which form from surface sites (nodes on the top surface layer) with a probability dependant on the applied potential and electrolyte concentration. The probability of surface pit formation is calculated in the same way as the probability of tip growth (explained latter) but is three orders of magnitude less for a potential parameter of the same value. Once a surface pit has formed the probability of pore growth in a time step, along any of the lattice lines, is determined by the potential and an electrolyte concentration parameter at the pore tip. The formation of new pore nodes produces a current j which flows along the channel connecting the pore tip to the surface. At the end of every time-step the overall current ι is calculated by the addition of current increment j from each new pore site.

As pore growth takes place ionic current passes through the channel connecting the pore tip to the surface causing a potential drop along the pore. The actual potential across the electrode-electrolyte interface at any pore tip is therefore reduced from the applied potential by the ohmic drop. The ohmic drop to a tip is calculated from the summation of the current flowing through each of the channel nodes connecting the tip to the surface, using the assumption that electrical resistance per node is constant along the pore length. Therefore the potential at a tip is:

$$\Psi_{Tip} = \begin{cases} A & if\ A \geq 0 \\ 0 & if\ A \leq 0 \end{cases} \quad \Big| \quad A = \Psi_{Surface} - \sum_{i=1}^{l} \left[r \sum_{n=1}^{N_i} j_{n,i} \right]$$

where Ψ_{Tip} and $\Psi_{Surface}$ are the electrode-electrolyte potentials at the tip and the surface respectively, r is the resistance per site, $j_{n,i}$ is the current passing through site i due to the

growth of pore tip n, N_i is the number of pore tips whose current passes through site i and l is the number of sites from pore tip to surface. $\Psi_{Surface}$ is taken to be equal to the applied potential.

The electrolyte concentration parameter is modeled by a simple diffusion of electrolyte through the pore channels. A finite difference method using the forward time centered space (FTCS) approximation [10,11] of the three-dimensional diffusion equation is used to calculate the diffusion of electrolyte through the pore structure. The effective diffusion coefficient of the electrolyte is determined by the values of λ and M. The finite difference method calculates diffusion by moving a fraction λ of the difference in concentration between two neighbouring sites from the high concentration site to the low concentration site. Each site can have a maximum of six neighbouring pore sites limiting the stability criterion of λ to less than 0.166. The value of λ used for all the results shown is 0.055. This process is repeated for a number of iterations M between pore growth time-steps. In the case of the basic algorithm the diffusion coefficient (i.e. the values of M and λ) is kept constant for a given simulation. The effect of varying the diffusion rate along the pores has also been investigated.

Growth is allowed at suitable active pore tips when the electrolyte concentration and node potential are greater than set threshold values. Where this is the case, the probability of growth at a site is calculated from the potential at the site as follows:

$$P_{Tip} = \left\{ \begin{array}{cc} 1 & if\ \Psi_{Tip}/\Psi_{Max} \geq 1 \\ \Psi_{Tip}/\Psi_{Max} & if\ \Psi_{Tip}/\Psi_{Max} \leq 1 \\ 0 & if\ \Psi_{Tip} \leq \Psi_{Min}\ \text{or}\ C_{Tip} \leq C_{Min} \end{array} \right\}, \Psi_{Tip} > \Psi_{Min}, C_{Tip} > C_{Min}$$

where P_{Tip} is the probability of growth, $\Psi_{Min} = 0.1$ is the threshold value of electrode-electrolyte potential needed for growth, C_{Tip} is the electrolyte concentration parameter at the tip, $C_{Min} = 1.5$ is the threshold value of C_{Tip} value needed for growth, and Ψ_{Max} is a constant set to a value of 0.6. To decide if growth can occur at a site a value between 0 and 1 is returned from a random number generator [9,10] and if this number is less than the value of P_{Tip} for that site a new pore tip is formed.

Active pore tips are those tips that are suitable for propagating further pore growth. The possibility of active pore tips existing at a pore site is decided by a number of factors. Electrochemical etching of InP by KOH is controlled by the tunneling of holes through the depletion layer at the electrode-electrolyte interface allowing a reaction such as the following to occur:

$$InP + 8OH^- + 8h^+ \rightarrow In^{3+} + PO_4^{3-} + 4H_2O$$

Therefore, since this limits the inter-pore wall thickness to the depletion layer width, active pore tips cannot exist on narrow inter-pore walls. Physically the geometry of the pore tip concentrates the electric field, increasing the probability of pore growth. Also, it is found experimentally that, at concentrations below 1.5 mol dm^{-3} KOH, porous growth does not occur and the formation of thin oxide films is observed on the surface. Where the concentration drops below this threshold value at a pore site, pore growth from a pore tip at that site could possibly be terminated through the modification of the tip geometry, reducing the electric field at the pore tip, or through the formation of a passivating film on the tip.

In the algorithm the deactivation of an active pore tip occurs if the electrolyte concentration fails to recover to a value greater than a threshold value within a short number of time-steps. Both the case of reversible and irreversible modification of the pore tips are investigated using the model. The probability of growth at a pore tip during its modification is calculated by the algorithm as follows:

$$P_{Film} = S \times P_{Tip} \quad , \quad S = \begin{cases} 1 & if\ \tau \le \tau_0 \\ 2 - (\tau/\tau_0) & if\ \tau_0 \le \tau \le 2\tau_0 \\ 0 & if\ \tau \ge 2\tau_0 \end{cases}$$

where P_{Film} is the probability of growth in the presence of a passivating film, τ_0 is a constant number of time-steps and τ is the number of time-steps for which the tip has been at a concentration below the threshold value, C_{Min}. (Note: The basic algorithm does not allow for a reduction in growth through the modification of pore tips.)

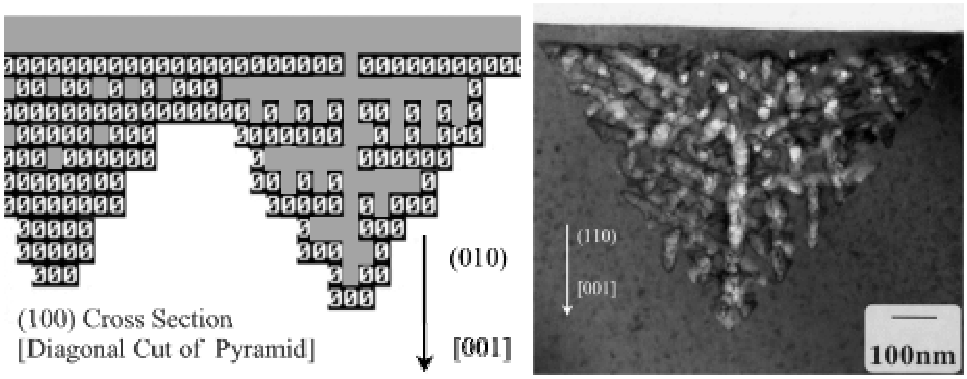


Fig. 1 (a) Initial structure formed prior to peak in current by a typical numerical simulation at an applied potential of 0.45 (KEY: 0 = InP depleted of carriers, White = Bulk InP, Grey = Pore) and (b) corresponding structure formed by electrochemical etching of InP during a linear potential seep from 0 to 0.44 V (SCE) in 5 mol dm^{-3} KOH at 2.5 mV s^{-1} in the dark.

RESULTS AND DISCUSSION

In Fig. 1, a typical porous structure formed initially during etching, in 5 mol dm^{-3} KOH is compared with a simulated structure created by the model. As expected, there is a strong resemblance between the initial porous domains formed experimentally and the structures which are simulated. The structures start from surface pits and grow along the <100> directions forming square-based pyramidal domains. The high potential at each of the pore tips allows pores to grow along all the <100> directions at an instantaneously equal rate causing regular domains to form and the number of active pore tips to increase rapidly. As these domains increase in size the concentration of electrolyte at the pore tips cannot be sustained by the diffusion of electrolyte from the surface pits and along the pores slowing down pore growth. The increase in the number of growing pore tips also increases the ohmic drops along the domain's pores. Different pore tips experience different ohmic drops which change continuously as the growth of new pores begin and end therefore with increasing domain size the ohmic drops experienced cause a greater spread of tip potentials. The effect of lower potentials with a wider distribution causes a range of low probabilities to be distributed at the pore tips producing a non-equal

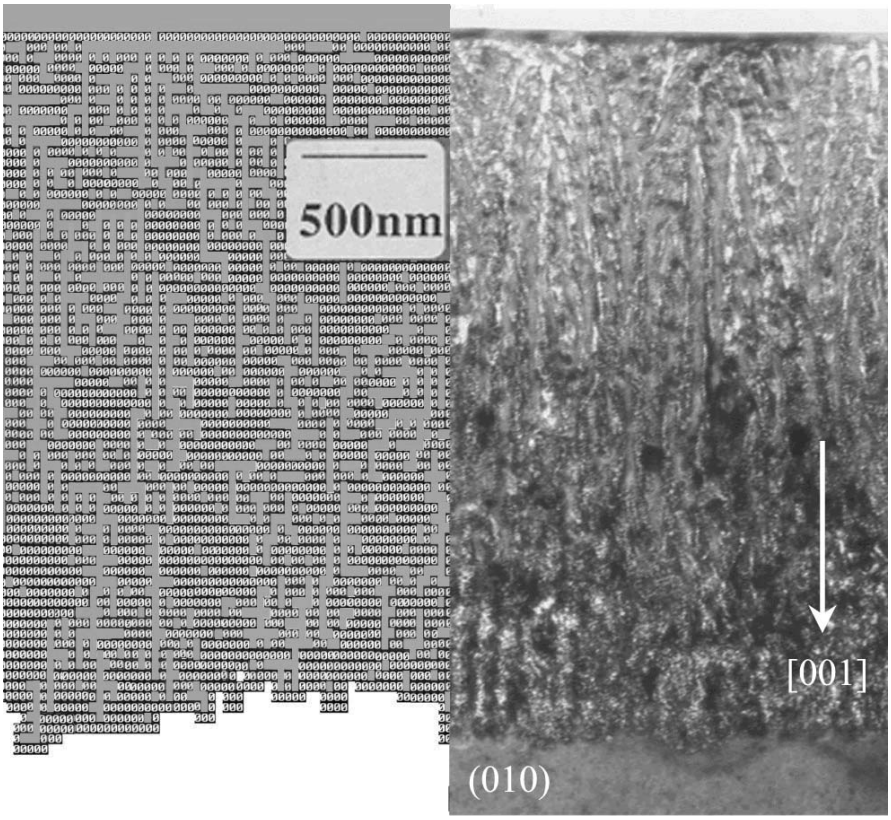


Fig. 2 Left: Cross-section of numerical structure formed for a potential of 0.45 at duration τ = 400 (KEY: 0 = InP depleted of carriers, White = Bulk InP, Grey = Pore). Right: TEM micrograph of InP anodized at 0.75 V (SCE) in 5 mol dm^{-3} KOH for 100 seconds.

instantaneous growth rate and allowing the domains to lose their regular shape. At extended durations of etching, after the merging of the porous domains, this non-equal instantaneous growth rate allows for the formation of a relatively flat porous to bulk interface similar to that found experimentally. Fig. 2 shows an example of the simulated structure formed at a potential of 0.45 and an experimental porous layer, formed at a constant potential of 0.75 V (SCE). These structures are created by the merging of porous domains after extended durations of etching.

Growth at a pore tip requires the electrolyte concentration to be above a threshold value C_{Min}. Since all the electrolyte that appears at the pore tips of a domain is diffused through the pores connecting the pore tips to the surface pit of that domain, the diffusion coefficient of the electrolyte should therefore have a large effect on growth rate and on the current versus time curves. Fig. 3 shows two sets of current versus time curves, which are typical of those produced by the basic numerical algorithm (the basic algorithm does not allow for the reduction of pore growth through the modification of pore tips) for a low and a high electrolyte diffusion coefficient. It can be seen from the graphs that the use of a lower electrolyte diffusion coefficient causes the current after the peak to fall off at a faster rate so that at longer times the currents at lower applied potentials have higher values than the currents at higher applied potentials. This effect is caused by simulations of higher applied potential producing a higher initial rate of etching and hence a higher rate of consumption of electrolyte. This causes the electrolyte concentrations to fall below C_{Min} sooner than in the case of low potential simulations, which use the same diffusion coefficient. However in simulations with high diffusion coefficients the current is not as strongly limited by diffusion but is predominantly affected by the ohmic drop due to an increase in resistance as pore length increases.

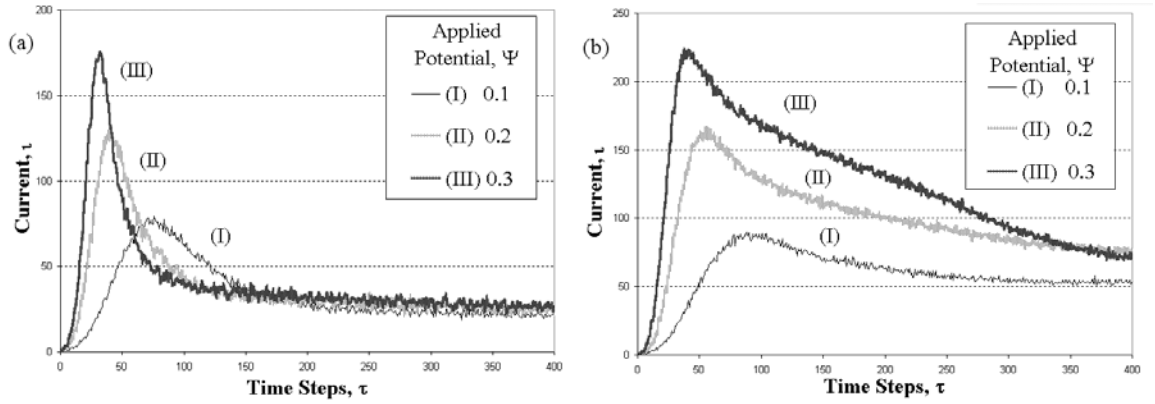


Fig. 3 Current versus time graphs simulated using the basic algorithm at three different values of constant potential (a) using a low diffusion coefficient (FTCS parameters: M = 50 and $\lambda = 0.055$) and (b) using a high diffusion coefficient (FTCS parameters: M = 500 and $\lambda = 0.055$).

When simulations at the same applied potential parameter, 0.1, but different diffusion coefficients are compared against each other (Fig. 4) a shortening in the number of time-steps before the peak in current, is observed, for lower electrolyte diffusion coefficients. Examination of these curves explains the experimental behaviour of current during initial etching. The initial rapid increase in current is caused by an expansion in the number of active pore tips as the domains spread out from the surface pits (as seen in Fig. 1). The current then peaks once the diffusion rate of electrolyte is no longer capable of sustaining the concentration at the pore tips above the threshold value for growth resulting in retardation in the growth of new pores. This can be concluded as the lowering of the diffusion coefficient causes the peaks to be limited to lower values of current and to occur at earlier times. The currents then decrease rapidly until a sustainable diffusion-consumption rate is attained producing a current that continues to gradually decrease as the average pore length increases. Diffusion of electrolyte is therefore a major controlling factor for pore growth rate and current: an increase in diffusion coefficient causes current peaks to increase in height, broaden and shift to later times and current values at extended durations to increase. It can also be seen that at sufficiently high diffusion coefficients the current becomes limited by the ohmic resistance rather than by the diffusion rate of electrolyte along the pores. For such simulations, the growth rate allowed by the maximum current through the pores is sustainable by the diffusion rate. Therefore no increase in current results from a further increase in diffusion coefficient.

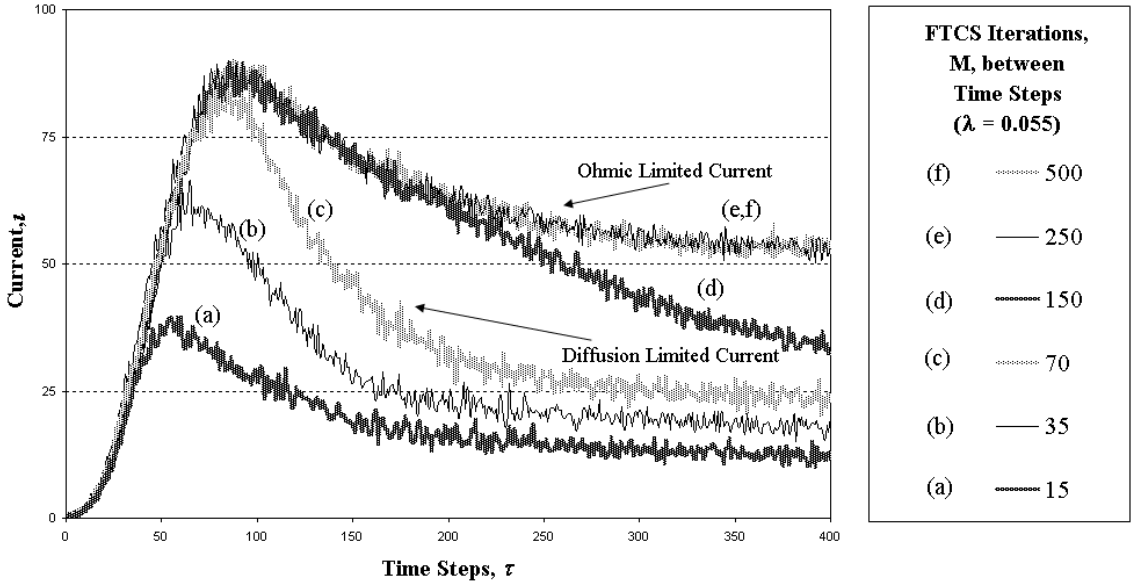


Fig. 4. Current versus time curves at a constant potential simulated using the basic algorithm at a range of different electrolyte diffusion coefficients. The coefficients are varied by changing the value of the FTCS parameter M. (The FTCS parameter λ is 0.055 and the applied potential is $\Psi = 0.1$.)

Experimental current versus time curves (Fig. 8) display the strongest agreement with simulated curves that use a low diffusion coefficient (Fig. 3a. FTCS parameters: λ = 0.055 and M = 50). Current peaks occur at earlier times, increase in height and narrow in width as applied potential is increased. At longer time durations this similarity between simulated and experimental curves is not maintained with the numerically simulated curves not falling uniformly to low currents as their experimental counterparts do.

It has been observed experimentally that below a threshold electrolyte concentration of 1.5 mol dm^{-3} KOH porous growth does not occur and instead the formation of thin oxide films on the InP surface is observed. The electrolyte concentrations in pores eventually drop below this threshold which could lead to the partial filling of the pores with oxide, reducing the diffusion rate of electrolyte. Simulations that allow for the partial filling of pores with oxide are shown in Fig. 5. The features of the curves at shorter times remain the same since the pore tips do not have electrolyte concentrations below the threshold value for oxide formation. The low diffusion rates through the partially oxide filled channels cause the currents to drop sharply after the peak to very low values. However, this drop in current manifests itself as a sharp decrease rather than the gradual decrease seen experimentally (Fig. 8). Furthermore the decrease in diffusion rate must be very large for such low currents to be reached.

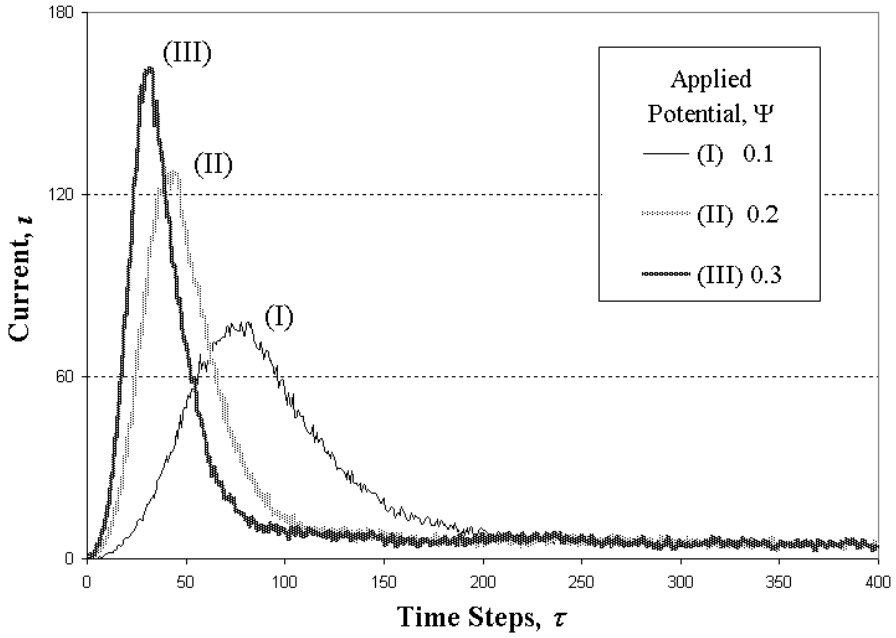


Fig. 5 Current versus time curves simulated at three different values of constant potential. The algorithm used allows for the formation of oxides which can partially fill the channels lowering the diffusion rate. (Diffusion rate reduced to 0.01 of its original value.) (FTCS parameters: M = 50 and λ = 0.055)

If the effect of electrolyte concentrations dropping below 1.5 mol dm^{-3} is to modify the pore tips through the formation of passivating films, the alteration of tip morphology or some other modification of the pore tip, this could possibly terminate pore growth. Fig. 6 shows simulated current versus time curves that are observed if passivating films are modeled to form at concentrations below a threshold value, C_{Min} = 1.5. It can be observed that the currents at different potentials merge to a similar current level after a common duration of etching before their currents continue to fall gradually in unison. This behaviour is similar to that seen experimentally (Fig. 8) but the simulated curves also display a recovery to higher current levels, which is most pronounced for an applied potential of 0.1. This effect is due to the recovery of electrolyte concentration at the pore tips which causes dissolution of the passivating film allowing for a burst in growth to occur.

It is possible that the modification of the pore tips by low electrolyte concentrations may be permanent, stopping pore growth from recovering even when higher electrolyte concentrations are regained. The simulated curves for such a mechanism of termination are shown for three different values of constant potential in Fig. 7 and are in strong agreement with typical experimental curves (Fig. 8). Both the experimental and simulated curves display currents that initially peak after different times before decreasing suddenly so as to merge and fall off gradually to very low currents at extended durations.

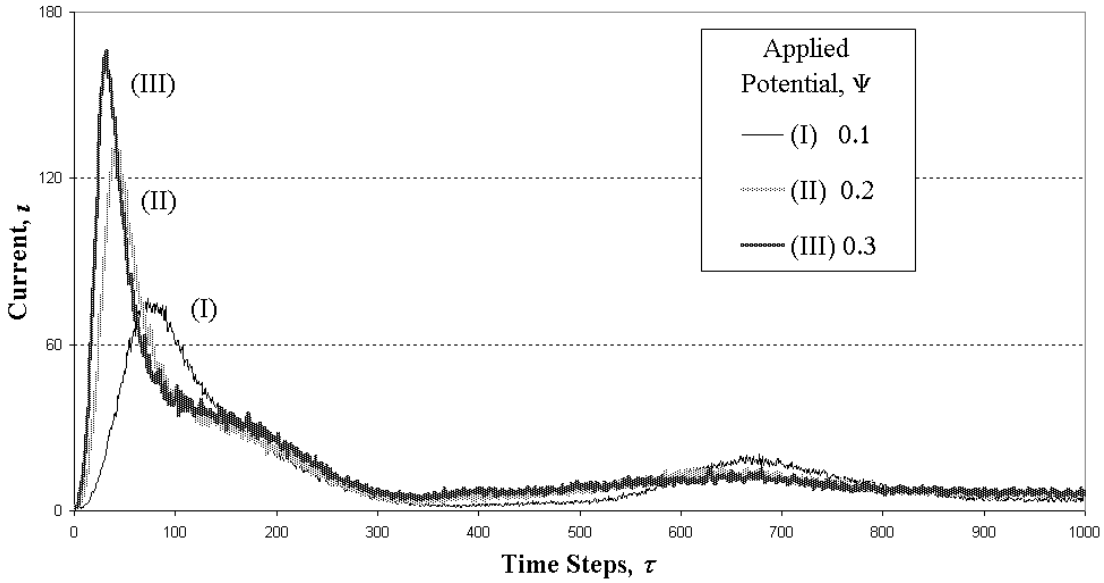


Fig. 6 Current versus time curves simulated at three different values of constant potential. The algorithm used allows for the formation of passivating layers at low electrolyte concentrations, which can re-dissolve when the electrolyte concentration recovers. (τ_0 = 7.5, FTCS parameters: M = 50 and λ = 0.055)

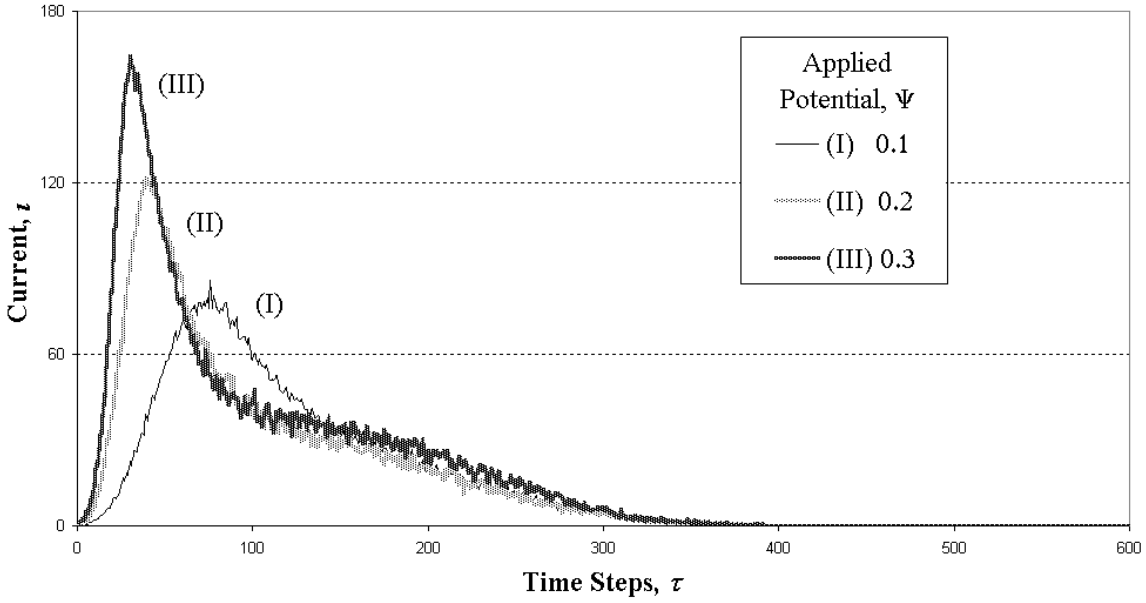


Fig. 7 Typical current versus time curves simulated for three different values of constant potential. The algorithm used allows for the termination of etching at pore tips by gradual irreversible modification of the active pore sites at electrolyte concentrations below C_{Min}. ($\tau_0 = 7.5$, FTCS parameters: M = 50 and $\lambda = 0.055$)

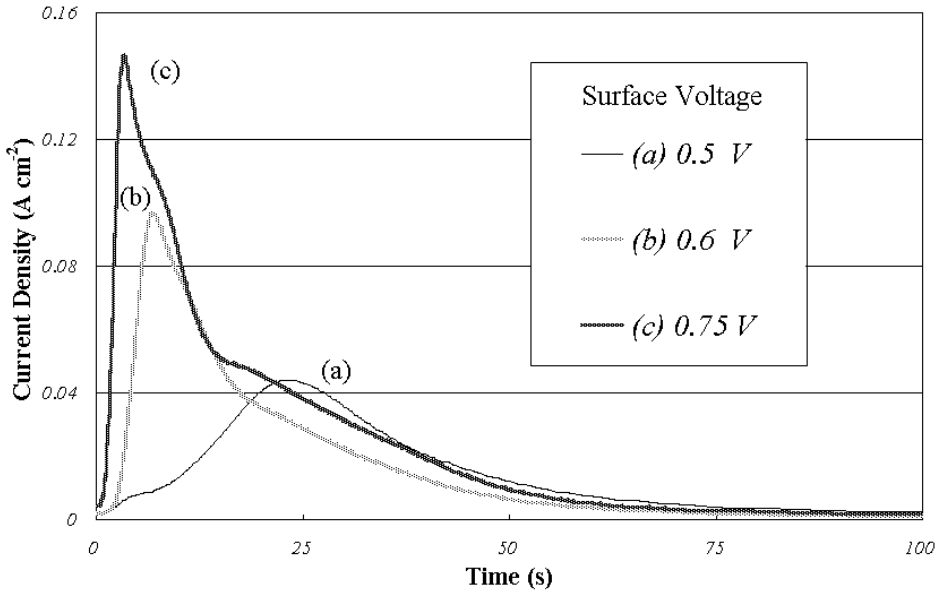


Fig. 8 Experimental current versus time curves for n-InP anodized in 5 mol dm^{-3} KOH in the dark at constant potentials of (a) 0.5 V (SCE) (b) 0.6 V (SCE) and (c) 0.75 V (SCE).

CONCLUSION

The process of porous growth in anodically etched n-type InP in 5 mol dm^{-3} KOH during the application of a potentiostatic voltage was modelled numerically. A mechanism of directional selectivity of pore growth preferentially along the <100> lattice directions was simulated and the results from these simulations were compared against experimental data. Experimentally pore growth creates nanoporous regions beneath a thin dense near-surface layer. In the early stages these regions take the form of square-based pyramidal domains originating at individual surface pits. Similar domains were produced by simulations which, at extended durations, merge together into a continuous layer with a relatively flat interface between the porous region and the substrate, comparable to that observed experimentally. The numerical current versus time curves produced also exhibit good agreement with experimental data. Manipulation of the parameters controlling these curves shows that the fall-off in current is controlled by the rate of diffusion of electrolyte through the pore structure with the final decline in current being caused by the termination of growth at the pore tips through the formation of passivating films or some other irreversible modification of the pore tips.

REFERENCES

[1] C. O'Dwyer, D.N. Buckley, *et al. Proceedings of the 37th State-of-the-Art Program on Compound Semiconductors*, PV 2002-14 p. 259 (ECS, 2002).

[2] C. O'Dwyer, D.N. Buckley, *et al. Proceedings of the 38th State-of-the-Art Program on Compound Semiconductors*, PV 2003-04 p. 63 (ECS, 2003).

[3] S. Langa, J. Carstensen, M. Christophersen, H. Föll, and I.M. Tiginyanu, *Appl. Phys. Lett.*, **78**, 1074 (2001).

[4] G. Oskam, A. Natarajan, P.C. Searson and F.M. Ross, *Appl. Surf. Sci*., **119** (1997) 160.

[5] S. Langa, J. Carstensen, I.M. Tiginyanu, M. Christophersen and H. Föll, *Electrochem. Solid-State Lett.*, **4** (2001) G50.

[6] S. Langa, I.M. Tiginyanu, J. Carstensen, M. Christophersen and H. Föll, *Electrochem. Solid-State Lett.* **3**, (2000) 514.

[7] R.L. Smith and S.D. Collins, *J. Appl. Phys*., **71**, 8 (1992).

[8] D. Stauffer. *J. Phys. A: Math. Gen.* **24** (1991) 909.

[9] D.E. Knuth, The Art of Computer Programming, Volume 2: Seminumerical Algorithms, p. 1-115 (Addison-Wesley, 1969)

[10] W.H. Press, S.A. Teukolsky, W.T. Vetterling and B.P.Flannery, Numerical Recipes in C 2nd Edition, p. 827-887 (Cambridge University Press, 1995)

[11] B. Gebhart, Heat Conduction and Mass Diffusion, p. 522-573 (McGraw-Hill, Inc., 1993).

[12] K. Hamamatsu, H. Kaneshiro, H. Fujikura and H. Hasegawa, *J. Electroanalytical Chem.*, **473** (1999) 223.